Design of High-Frequency Gm-C Wavelet Filters

Wenshan Zhao[1, 2], Yichuang Sun[1], Xi Zhu[1], and Yigang He[2]

1. School of ECEE, University of Hertfordshire, Hatfield, Herts AL10 9AB, UK

2. College of Electrical & Information Engineering, Hunan University, Changsha, Hunan 410082, China

Email: shmilyzhyao@yahoo.com.cn, Y.Sun@herts.ac.uk

Abstract—**A high–frequency wavelet filter which employs Gm–C blocks based on leap–frog (LF) multiple–loop feedback (MLF) structure is presented. The proposed method is well suitable for high–quality high–frequency operation since the Gm–C based filter can achieve high frequency, whilst LF MLF configuration has the characteristics of lower magnitude sensitivity and capability of realizing arbitrary rational functions. The Marr wavelet is selected as an example in this paper, and the design for a 100MHz frequency operation is elaborated. The wavelet filter is simulated using TSMC 1.8V 0.18μm CMOS technology. Simulation results indicate that the proposed method is feasible for high frequency operation with relatively low power consumption.**

I. INTRODUCTION

Wavelet transform (WT) has found a wide range of applications in signal processing, particularly for local analysis of non–stationary and fast transient signals, due to its time–frequency localization characteristics [1]. In order to achieve real–time performance, hardware implementations of WT have been investigated over the past few years, which often employ digital circuitry. As analogue circuits have the characteristics of low power dissipation and high–speed compared with digital circuits, wavelet implementations using analogue circuits have attracted much attention. However, research in this so far has mostly concentrated on audio–frequency operations such as biomedical implantable devices [2-7]. In recent years, WT has also been shown to be a very promising mathematical tool for high–frequency signal processing, e.g. modulation identification for communications [8], target detection in radar signal processing [9], and partial discharge detection and classification [10]. Thus, analogue wavelet transform circuits for high–frequency applications must also be investigated. The aim of this paper is therefore to propose a method for analogue implementation of WT for high–frequency operation.

As of now, the prevalent methods for analogue implementation of WT have mainly focused on the mathematical approximation of wavelet bases and the design of bandpass filters whose impulse responses are the approximated wavelet bases (i.e. wavelet filters) [4-7]. Since there have already been many approaches for wavelet base approximation, this paper will only pay attention to the design of wavelet filters. As for the high–frequency operations, the Gm–C based bandpass filter is the most popular technique so far as its center frequency can reach a few hundred megahertz [11]. Meanwhile from the viewpoint of filter synthesis, many filter architectures such as cascade and LC ladder simulation have been utilized in analogue wavelet filters. Although successful in many aspects, these designs suffer from the effect of higher magnitude sensitivity (cascade) and incapability of realizing real zeros directly (LC ladder simulation). It has been demonstrated that the multiple–loop feedback (MLF) approach does not have these problems [12].

To obtain a high–quality high–frequency wavelet filter, an analogue bandpass filter which employs Gm–C blocks based on the leap–frog (LF) MLF structure is proposed in this paper. Also, to reject even–order distortion and optimize linearity, a fully–differential linear transconductor is used as the Gm cell in this bandpass filter. The paper takes the Marr wavelet (i.e. Mexican hat wavelet) for example to elaborate the proposed approach. The feasibility of the method is confirmed by simulation results.

II. WAVELET DESIGN PROCEDURE

Wavelet analysis is performed by decomposing a signal into components appearing at different scales. Assuming $\psi(t)$ is wavelet base (or mother wavelet), the wavelet transform of the signal $x(t)$ can be defined by convolving $x(t)$ with a dilated wavelet [1],

$$WT_x(a,b) = \frac{1}{a}\int x(t)\psi(\frac{b-t}{a})dt \qquad (1)$$

where a and b are respectively the scale parameter and time–shift. The coefficient, $1/a$, maintains the amplitude of frequency response of $\psi_{a,b} = \frac{1}{a}\psi(\frac{b-t}{a})$ across different scales. Hence, the WT can be carried out simply by using a filter with a dilated impulse response (defined by $\psi(t)$).

Generally, the prevalent design procedure for analogue implementation of WT is summarised as: mathematically approximate the wavelet bases with realizable rational expressions and then implement them using suitable circuit topologies which act as bandpass filters (i.e. wavelet filters). Several mathematical techniques have been provided to achieve the best possible approximation. In [7], a wavelet design method based around the mathematical approximation of wavelet bases is presented to obtain an optimal WT

implementation. Herein, the optimal approximation for Marr wavelet provided in [7] is used as an example to illustrate the wavelet filter design.

III. WAVELET FILTER DESIGN

A. Design of the Gm Cell

The Gm–C technique is widely regarded as the optimum option for CMOS integrated high–frequency continuous–time filters [11]. The performance of a Gm–C block relies heavily upon the characteristics of the transconductor employed. To optimize the linearity and DC gain, this paper uses the transconductor proposed in [13] with active biasing and a negative compensation load (G_L) implemented using the same transconductor, as shown in Fig. 1.
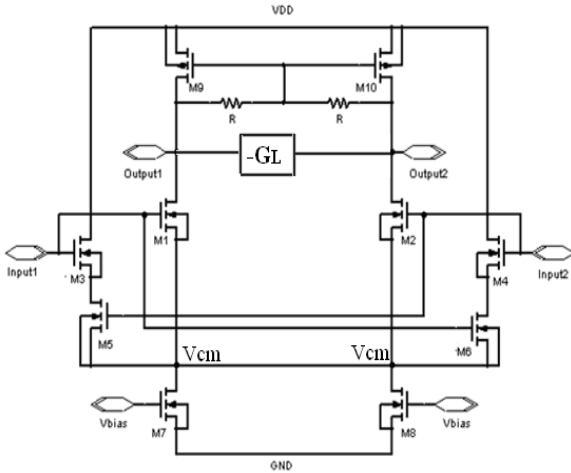

Figure 1. Schematic of the Gm cell.

In the Gm cell, M_1 and M_2 act as the input transistors. The differential pair M_3–M_6 acts as the active biasing circuitry in such a way that the total bias current drawn by M_3–M_6 is less for larger signals. It shares the same bias current source with the differential pair M_1–M_2. When the signal amplitude is small, M_5 and M_6 are in triode region while M_3 and M_4 are in saturation. The M_3–M_6 branches take away some of the bias current. When the signal amplitude is positive and large, M_5 will be cut off and M_6 will become saturated. A smaller proportion of the total bias current will be drawn by M_3–M_6. This leads to larger currents in M_1 and M_2 to compensate for the drop of the transconductance. The sizing of the transistors must be optimized for maximum linearity [13].

Let $K_{3,4}$ be C times of $K_{5,6}$ for higher linearity, where $K_x = \mu C_{ox} W_x / L_x$. Based on the analysis above, I_{D3} and I_{D5} have the following relationship

$$I_{D3} = I_{D5} \Rightarrow 0.5K_3(0.5V_{in} - V_{d5} - V_t)^2$$
$$= K_5[-(0.5V_{in} + V_{cm} + V_t)V_{ds5} - 0.5V_{ds5}^2] \quad (2)$$

Let $V_{cm} + V_t = V_{cm}^*$, I_{D3} can be written as

$$I_{D3} = K_3[0.5V_{in} - (V_{ds5} + V_{cm}^*)]^2$$
$$= \frac{K_3}{4(C+1)^2}[2V_{in} - \sqrt{(1-3C)V_{in}^2 + 4(C+1)V_{in}V_{cm}^* + 4(C+1)V_{cm}^{*2}}]^2 \quad (3)$$

I_{D4} has a similar expression except with V_{in} being replaced by $-V_{in}$. Therefore, the output current can be expressed as:

$$I_{out} = K_{1,2}\sqrt{\frac{I_B - [0.5K_{1,2} - \frac{K_{3,4}}{2(C+1)^2}(5 - 3C - 4\sqrt{C+1})]V_{in}^2}{2[K_{1,2} + (C+1)K_{3,4}]}} V_{in} \quad (4)$$

where I_B is the bias current.

Using Taylor series expansion, (4) can be written as

$$I_{out} \approx \sqrt{\frac{K_{1,2}^2 I_B}{2[K_{1,2} + (C+1)K_{3,4}]}} V_{in} - \frac{K_{1,2}^2 - \frac{K_{1,2}K_{3,4}}{(C+1)^2}(3C + 4\sqrt{C+1} - 5)}{12\sqrt{2[K_{1,2} + (C+1)K_{3,4}]I_B}} V_{in}^3 \quad (5)$$

Note that the even–order harmonic distortions are cancelled completely due to the symmetry of fully–differential Gm cell. The total harmonic distortion is mainly determined by the third harmonic distortion (HD3). As seen from (5), HD3 can be cancelled as long as the following relationship is met,

$$K_{1,2}^2 = \frac{K_{1,2} \cdot K_{3,4}}{(C+1)^2}(3C + 4\sqrt{C+1} - 5) \quad (6)$$

The value of variable C is chosen to give an optimal value of linearity.

Therefore, the transconductance of this Gm cell shown in Fig. 1 is derived as

$$G_m \approx \sqrt{\frac{K_{1,2}^2 I_B}{2[K_{1,2} + (C+1)K_{3,4}]}} \quad (7)$$

The differential loading R is made with two polysilicon resistors for better linearity and more constant loading toward different signal swings. A negative Gm cell ($-G_L$) is connected in parallel to the transconductor output to enhance the output impedance. The design of the $-G_L$ cell is similar to that of the Gm cells except that the outputs are cross coupled to the inputs.

B. Filter Architecture and Synthesis

The filter's performances not only rely on the characteristics of transconductors, but also strongly on the filter structure. Due to the feature of lower magnitude sensitivity and capability of realizing arbitrary rational function directly, the LF MLF configuration is used for the filter design.

The normalized approximation function for Marr wavelet at a=0.100 proposed in [7] is given as:

$$H(s) = \frac{-6.88 \times 10^{-3} s^2}{D(s)} \quad (8)$$

Where $D(s) = 2.34 \times 10^{-8} s^7 + 1.34 \times 10^{-6} s^6 + 3.70 \times 10^{-5} s^5 +$

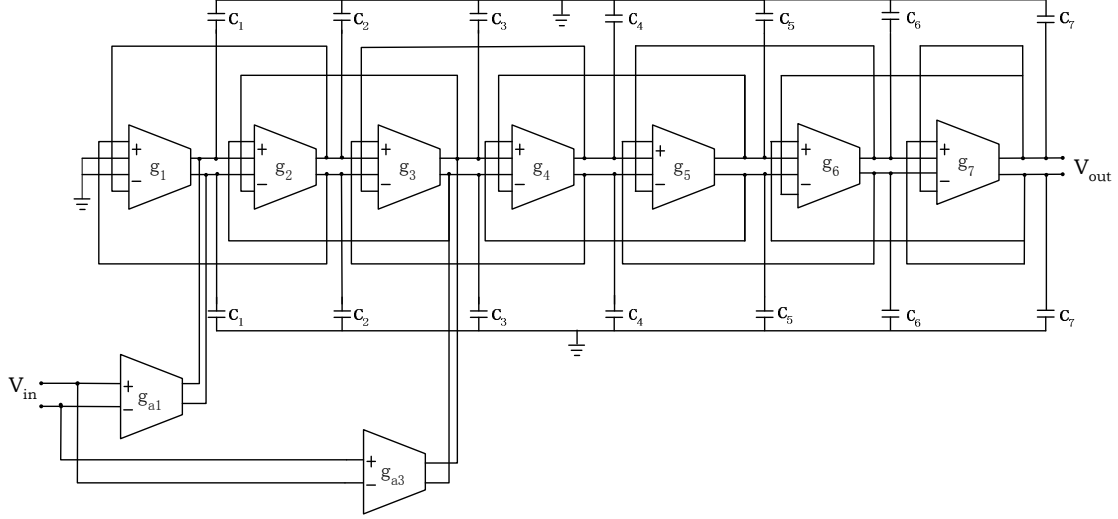$$6.79 \times 10^{-4} s^4 + 8.67 \times 10^{-3} s^3 + 0.075 s^2 + 0.40 s + 1$$

Figure 2. Fully-differential LF bandpass filter with input distribution transconductor network.

By adding the input distribution transconductors network to produce zeros, the fully-differential realization of (8) using the LF MLF architecture is shown in Fig. 2.

Denoting $\tau_j = C_j / g_j$ and $\beta_j = g_{aj} / g_j$, the overall transfer function of the filter can be derived as

$$H(s) = \frac{V_{out}}{V_{in}} = \frac{N(s)}{D(s)} \qquad (9)$$

Where $N(s) = \beta_3 \tau_2 \tau_1 s^2 + (\beta_3 + \beta_1)$

$D(s) = \tau_7 \tau_6 \tau_5 \tau_4 \tau_3 \tau_2 \tau_1 s^7 + \tau_6 \tau_5 \tau_4 \tau_3 \tau_2 \tau_1 s^6 +$
$(\tau_7 \tau_6 \tau_3 \tau_2 \tau_1 + \tau_5 \tau_4 \tau_3 \tau_2 \tau_1 + \tau_7 \tau_6 \tau_5 \tau_4 \tau_1 +$
$\tau_7 \tau_6 \tau_5 \tau_2 \tau_1 + \tau_7 \tau_4 \tau_3 \tau_2 \tau_1 + \tau_7 \tau_6 \tau_5 \tau_4 \tau_3) s^5 +$
$(\tau_4 \tau_3 \tau_2 \tau_1 + \tau_6 \tau_5 \tau_4 \tau_3 + \tau_6 \tau_5 \tau_2 \tau_1 + \tau_6 \tau_3 \tau_2 \tau_1$
$+ \tau_6 \tau_5 \tau_4 \tau_1) s^4 + (\tau_5 \tau_2 \tau_1 + \tau_3 \tau_2 \tau_1 + \tau_7 \tau_6 \tau_5 +$
$\tau_7 \tau_6 \tau_3 + \tau_5 \tau_4 \tau_3 + \tau_5 \tau_4 \tau_1 + \tau_7 \tau_2 \tau_1 + \tau_7 \tau_6 \tau_1 +$
$\tau_7 \tau_4 \tau_3 + \tau_7 \tau_4 \tau_1) s^3 + (\tau_6 \tau_1 + \tau_4 \tau_3 + \tau_6 \tau_3 +$
$\tau_4 \tau_1 + \tau_6 \tau_5 + \tau_2 \tau_1) s^2 + (\tau_7 + \tau_5 + \tau_3 + \tau_1) s + 1$

Using the coefficient matching between (8) and (9), the parameter values can be calculated as:

$$\tau_1 = 0.17654, \ \tau_2 = 0.12312 \ , \tau_3 = 0.11831 \ ,$$
$$\tau_4 = 0.11151 \ , \tau_5 = 0.08769 \ , \tau_6 = 0.05330, \qquad (10)$$
$$\tau_7 = 0.01746, \ \beta_1 = 0.31654 \ , \beta_3 = -0.31654$$

To improve transconductors matching and facilitate design automation, identical Gm cells are employed in the filter design. One can denormalize (8) to any desired centre frequency according to application requirement. For example, the frequency bandwidth using WT in [10] is from 20MHz to 200MHz which is determined by the frequency range of

biconical antenna. Herein, the centre frequency is selected around 100MHz. Choosing 1.4mS for the transconductance of identical Gm cells in integrators, the transconductance g_{a1} and g_{a3} of the input transconductors can be obtained by (10) as 0.948mS and –0.948mS respectively, in which the negative transconductance can be realized simply by exchanging the input terminals of the transconductor. It is interesting to note that the realization of the bandpass Marr wavelet characteristic of (8) requires $g_{a1} = -g_{a3}$. This shows the simplicity of realization and is also a desired feature for IC design due to the identical value.

Also, the capacitors values, with parasitic capacitance 0.2pF taken into account, can be calculated by (10) as below

$$C_7 = 2.2122\,pF, C_6 = 3.3639\,pF, C_5 = 5.5347\,pF,$$
$$C_4 = 7.0380\,pF, C_3 = 7.4673\,pF, C_2 = 7.7708\,pF, \qquad (11)$$
$$C_1 = 11.1429\,pF$$

IV. SIMULATION RESULTS

The wavelet filter is designed and simulated using TSMC 0.18μm CMOS technology with 1.8V power supply. Fig. 3 depicts the frequency response of the filter simulated by HSpice, achieving the peak value 0.576 at f=100MHz. The –3dB frequencies of this filter are 75.6MHz and 118MHz respectively, which are almost the same as the ideal values. As seen from Fig. 3, the performance of the Gm–C wavelet filter is confirmed by the excellent approximation of the Marr wavelet. Simulation results have shown a total harmonic distortion (THD) of less than -40dB for 240 mV$_{pp}$ differential input signal. The input equivalent noise is 18.2 nV/$\sqrt{\text{Hz}}$ at 100 MHz, corresponding to a dynamic range of about 56 dB. The total power consumption of the filter is about 41.2mW.

By changing the transconductance values gi, or capacitance values Ci, the wavelet system composed of wavelet filters at different scales can be implemented

accordingly. Fig. 4 plots the frequency responses of the wavelet filter at two other scales a=0.5 and a=0.05, whose centre frequency is 20MHz and 200MHz respectively. Observed from these figures, the wavelet filter proposed in this paper works well in high and very high frequencies.
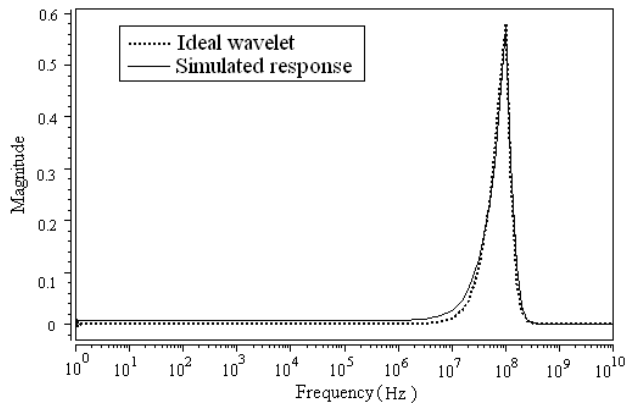

Figure 3. Frequency response of the wavelet filter with *a*=0.1.
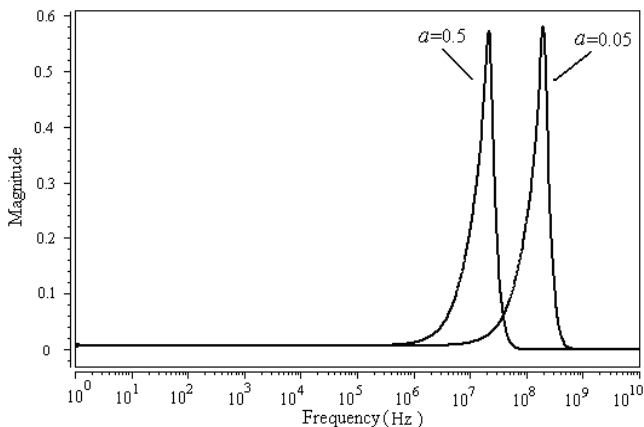

Figure 4. Frequency response of the wavelet system with *a*=0.5 and *a*=0.05.

V. CONCLUSIONS

To meet the requirement for high–frequency real–time application of wavelet transform, a novel analogue wavelet filter which employs Gm–C blocks based on LF MLF structure is presented. A fully–differential linear transconductor is utilized as the Gm cell to enhance the wavelet filter's performance. The proposed approach is described by taking the Marr wavelet base as an example. The wavelet filter is designed for 20MHz–200MHz frequencies and simulated using 1.8V 0.18μm CMOS technology. Simulation results show an excellent approximation of the Marr wavelet base with only 41.2mW power dissipation. This research demonstrates that the proposed wavelet filter can achieve high frequency with relatively low power consumption and is well suited for analogue implementation of wavelet transform for high–frequency applications.

REFERENCES

[1] S. Mallat, A Wavelet Tour of Signal Processing. New York: Academic Press, 2001.

[2] J. Lin, W. H. Ki, T. Edwards, and S. Shamma, "Analog VLSI implementations of auditory wavelet transforms using switched-capacitor circuits," IEEE Trans. Circuits and Syst., Vol. 41, No. 9, pp. 572-583, 1994.

[3] R. T. Edwards and C. Cauwenberghs, "A VLSI implementation of the continuous wavelet transform," Proc. IEEE ISCAS, pp.368-371, 1996.

[4] Moreira-Tamayo and de Gyvez J. Pineda, "Analog computation of wavelet transform coefficients in real-time," IEEE Trans. Circuits and Syst., Vol. 44, No. 1, pp. 67-70, 1997.

[5] S. A. P. Haddad, R. Houben, and W. A. Serdijn, "Analog wavelet transform employing dynamic translinear circuits for cardiac signal characterization," Proc. IEEE ISCAS, Vol. 1, pp. 121-124, 2003.

[6] S. A. P. Haddad, S. Bagga, and W. A. Serdijn, "Log-domain wavelet bases," IEEE Trans. Circuits and Syst., Vol. 52, No. 10, pp. 2023-2032, 2005.

[7] A. J. Casson, D. C. Yates, S. Patel, and E. Rodriguez-Villegas, "An analogue bandpass filter realization of the continuous wavelet transform," Proc. IEEE EMBS, pp. 1850-1854, 2007.

[8] K. C. Ho, W. Prokopiw, and Y. T. Chan, "Modulation identification of digital signals by the wavelet transform," IEE Proc.- Radar, Sonar Navig., Vol. 147, No. 4, pp. 169-176, 2000.

[9] E. Elsehely and M. I. Sobhy, "Real time radar target detection under jamming conditions using wavelet transform on FPGA device," Proc. IEEE ISCAS, pp. 545-548, 2000.

[10] M. Kawada, A. Tungkanawanich, Z. I. Kawasaki, and K. Matsu-ura, "Detection of wide-band E-M signals emitted from partial discharge occurring in GIS using wavelet transform," IEEE Trans. Power Delivery, Vol. 15, No. 2, pp. 467-471, 2000.

[11] Y. Sun, Design of High Frequency Integrated Analogue Filters. Stevenage: IEE Press, 2002.

[12] Y. Sun, "Synthesis of leap-frog multiple-loop feedback OTA-C filters," IEEE Trans. Circuits and Syst., Vol. 53, No. 9, pp. 961-965, 2006.

[13] C. S. Kim, Y. H. Kim, and S. B. Park, "New CMOS linear transconductor," Electron. Letter, Vol. 28, No. 21, pp. 1962-1964, 1992.